CLM-P715

CLM-P715

UKAEA

Preprint

IDEAL MHD BALLOONING INSTABILITY AND SCALING LAW FOR CONFINEMENT

J. W. CONNOR
J. B. TAYLOR
M. F. TURNER

CULHAM LABORATORY
Abingdon Oxfordshire
1984

CLM-P 715

IDEAL MHD BALLOONING INSTABILITY AND SCALING LAW FOR CONFINEMENT

J W Connor, J B Taylor, M F Turner

Culham Laboratory, Abingdon, OX14 3DB, England

(Euratom/UKAEA Fusion Association)

Abstract

The confinement time for an ohmically heated, low-β, tokamak is well described by the scaling law $\tau \propto n$. This implies that β should increase linearly with additional auxiliary heating power. In fact the increase is much slower, and confinement deteriorates with increasing auxiliary heating. We examine the possibility that this deterioration is due to the localised onset of mhd ballooning instabilities, with confinement elsewhere continuing to follow the law established for ohmic discharges. We find that the overall effect of the ballooning instability is indeed gradual and the resultant confinement time corresponds to a scaling law in good agreement with that reported for auxiliary heated tokamaks.

(Submitted for publication in Nuclear Fusion)

January 1984

I. Introduction

The confinement time of an ohmically heated, low-β, tokamak is well described[1] by the scaling law $\tau \propto n$, where n is the plasma density. If this were also true for tokamaks with auxiliary heating we would expect the plasma β to increase linearly with the additional power P. However, a number of experiments show a saturation of β with increasing P, which can be interpreted as a deterioration in confinement at higher values of β. There is, of course, a theoretical prediction[2] of a maximum attainable β, set by ideal mhd ballooning instabilities, but it is unlikely that experiments have reached this limit - which correspond to an optimised pressure profile marginally stable at each point[3].

In this note we examine the possibility that the observed deterioration in confinement arises because the pressure gradient has reached the ballooning stability limit only in some limited region. In this region the confinement is degraded, but elsewhere it still follows the form established for low-β ohmic plasmas.

In section II we describe a model representing this behaviour. In it the thermal conductivity χ is proportional to $1/n$ wherever the pressure gradient is less than that for onset of local ballooning modes; where this limit is exceeded the conductivity is effectively infinite so that the pressure gradient remains at the marginal value. With increasing power input the stable regions shrink and overall confinement gradually deteriorates. The magnetic field is consistently determined from Ohm's law and the effect of "sawtooth" oscillations is simulated by imposing a flat pressure profile within the $q = 1$ surface.

In section III we discuss the results calculated for this model and show that they correspond to scaling laws very similar to those quoted for high-β auxiliary heated tokamaks.

II. The Transport Model

Where ballooning modes are stable we take the thermal conductivity to have the form

$$\chi = \chi_I = 5.10^{19}/n \quad m^2 sec^{-1} \tag{1}$$

established empirically for ohmic discharges and widely used, eg in INTOR studies. For simplicity we assume n is independent of radius and concentrate on the heat transport processes. Then in a cylindrical approximation the thermal conduction equation for the temperature T can be written

$$\frac{1}{r}\frac{d}{dr} r\chi_I \frac{dp}{dr} + H(r) = 0 \tag{2}$$

where $H(r)$ is the heating power density and $p = 2nT$ is the pressure.

Ballooning instabilities set a limit to the pressure gradient beyond which Eq (1) is no longer applicable. For a large aspect ratio tokamak with circular magnetic surfaces this maximum pressure gradient, as given in Ref 4, is

$$\frac{-2Rq^2}{B_0^2}\frac{dp}{dr} = f(s) \qquad (3)$$

where $q = rB_0/RB_\theta$ and $f(s)$ is a function of the magnetic shear $s \equiv (r/q)(dq/dr)$ shown in Fig 1. [This is a more accurate recalculation of the figure in Ref 4.] In our model, the pressure gradient is determined by Eq (2) so long as it lies below the threshold set by Eq (3), (the mhd stable zone). Elsewhere the pressure gradient takes the threshold value itself (the mhd unstable zone): this represents a transport coefficient which increases by a large factor once the threshold gradient is exceeded.

The shear s appearing in Eq (3) is related to the pressure profile through Ohm's law and the equation for the poloidal field:

$$\frac{1}{r}\frac{d}{dr} rB_\theta = \sigma E \qquad (4)$$

since (in our model with uniform density) the conductivity σ is proportional to $p^{3/2}$.

Finally, in order to simulate the rapid energy transport accompanying sawtooth oscillations we set the pressure gradient to zero everywhere inside the radius at which $q(r) = 1$. This vanishing pressure gradient implies (through Eq (4)) that the current is uniform and so $q = 1$ throughout this internal region. Elsewhere the current, field and pressure profiles adjust according to the transport and ballooning stability equations and Ohm's law.

Our model therefore has several zones; (i) an inner sawtooth zone in which $q = 1$ and $dp/dr = 0$, (ii) transport zones, in which dp/dr is determined by Intor-like heat transport, Eq (2), and (iii) ballooning zones in which dp/dr is determined by the ballooning stability criterion Eq (3). The boundary conditions are $dp/dr = 0$ at $r = 0$ and $p = 0$ at $r = a$. A further condition on dp/dr is needed at the inner boundary of a transport zone (whenever this is not at $r = 0$). Here the heat flow is continuous but dp/dr may not be, and the required condition is that dp/dr be consistent with the power deposited inside the zone boundary. These conditions completely specify the problem for any given heating profile.

It is convenient to introduce dimensionless variables

$$x = \frac{r}{a} \quad , \quad \frac{p(r)}{p(o)} = \tilde{p}(x) \quad , \quad \frac{B_\theta(r)}{B_\theta(a)} = b(x) \quad , \quad \frac{4\pi^2 R a^2 H(r)}{P} = h(x)$$

(so that $\int_0^1 h(x)\ x\ dx = 1$). Then the confinement time is

$$\tau = \frac{3}{2} \frac{4\pi^2 a^2 R p_0}{P} \int_0^1 \tilde{p}(x)\ x\ dx \qquad (5)$$

where P is the total input power. If the ballooning instability were ignored the "Intor" confinement time would be

$$\tau_I = \frac{3c}{2} \frac{a^2}{\chi_I} \qquad (6)$$

where c depends on the heating profile;

$$c = \frac{1}{4}\left\{1 - \left(\int_0^1 h(x)\ x^3\ dx\right)\right\} \tag{7}$$

In terms of the dimensionless variables the equations of our model become:

$$\frac{1}{x}\frac{d}{dx}\left(x\frac{d\tilde{p}}{dx}\right) + \frac{1}{\lambda}h(x) = 0 \tag{8}$$

for the pressure gradient in the stable zones;

$$\frac{-A\lambda x^2}{b^2}\frac{d\tilde{p}}{dx} = f(s) \tag{9}$$

for the pressure gradient in the ballooning unstable zones;

$$\frac{d\tilde{p}}{dx} = 0 \quad \text{when} \quad \frac{x}{b} < \frac{RB_\theta(a)}{aB_0} \tag{10}$$

for the pressure gradient in the sawtooth oscillation zone; and

$$\frac{1}{x}\frac{d}{dx}(xb) = \tilde{p}^{3/2}\left(\int_0^1 \tilde{p}^{3/2} x dx\right)^{-1} \tag{11}$$

for the poloidal magnetic field. These equations involve only the parameters

$$\lambda \equiv c \frac{\tau}{\tau_I} \left(\int_0^1 \tilde{p} x dx \right)^{-1} \tag{12}$$

$$A \equiv \frac{4}{3c} \frac{Pa}{I^2 R^2} \tau_I \tag{13}$$

and

$$q_a \equiv \frac{aB_0}{RB_\theta(a)} \quad . \tag{14}$$

For any given heating profile one can compute λ, and hence τ/τ_I as a function of the two parameters A (which measures the power input) and q_a (the safety factor). Equally one may compute β as a function of A and q_a through the relation

$$\beta = 2c \frac{A\tau}{\tau_I} \beta_c$$

where $\beta_c \equiv a/Rq_a^2$.

III. Results and Discussion

In this section we consider the variation of τ/τ_I and β/β_c with the power input A and safety factor q_a, computed for two heating profiles. The first is a uniform heat deposition, $h(x)$ = constant, and the second a centrally peaked profile $h(x) = \exp(-2.77x^2)$. In each case the stability boundary for ballooning modes is taken from Fig 1. For each value of A and q_a, the solution is computed by a two-stage iteration procedure. From a pressure profile $\tilde{p}_m(x)$ a magnetic field $b_m(x)$ is

computed using Eq (11). Then, with this $b_m(x)$ held fixed, a new $\tilde{p}(x)$ and an interim eigenvalue λ is computed from Eqs (8), (9) and (10) by an iterative-shooting method. When this inner loop has adequately converged this new $\tilde{p}(x)$ $\left(\equiv \tilde{p}_{m+1}(x)\right)$ replaces $\tilde{p}_m(x)$ in the outer iteration until both $\tilde{p}_m(x)$ and $b_m(x)$ are sufficiently well converged.

The computed values of τ/τ_I and β/β_c are shown in Figs 2-5 and are similar for the two heating profiles. The onset of ballooning instability produces a reduction in confinement time but β continues to rise - as shown in Figs 4 and 5.

The underlying reduction in confinement time, due to ballooning instability, is most clearly shown by the curves for large q_a. These correspond to the behaviour in the absence of sawtooth activity. At smaller q_a there is an additional degradation in confinement at high power levels due to sawtooth activity; the power level at which this sets in decreases as q_a is reduced. For the case $q_a = 2.5$ the additional degradation is more marked because sawtooth activity sets in even before ballooning influences confinement.

It is interesting to infer a confinement time scaling from these results. Fig 6 shows a logarithmic plot of the calculated confinement times. It can be seen that, over a considerable range, the confinement time can be represented as

$$\frac{\tau}{\tau_I} \propto A^{-\gamma} \qquad (15)$$

with $\gamma \approx 0.72$. Introducing τ_I from Eqs (1) and (6), ie

$$\tau_I = 3c\ 10^{-20}\ n(m^{-3})\ a^2(m) \quad , \qquad (16)$$

implies that for confinement of high-β tokamaks

$$\tau \propto n^{1-\gamma}\ I^{+2\gamma}\ P^{-\gamma}\ a^{2-3\gamma}\ R^{+2\gamma} \qquad (17)$$

or, with $\gamma = 0.72$,

$$\tau \propto n^{0.28}\ I^{1.44}\ P^{-0.72}\ a^{-0.16}\ R^{1.44} \quad . \qquad (18)$$

This is in remarkably good agreement with the empirical scaling laws reported[1] for tokamaks with high-power auxiliary heating. It should be noted that although this scaling law differs considerably from the intrinsic Intor scaling, it has been derived from Intor without any adjusted parameters. [As indicated earlier, these results are based on a model with uniform density. In a similar model with density at the wall ~ 10% of its central value the index γ ranged from 0.72 to 0.80.]

Figs 4 and 5 show that saturation of β with increasing input power commences at $A \approx 1$. In terms of experimental parameters

$$A = \frac{3.2\ 10^{-20}\ n(m^{-3})\ P(MW)\ a^3(m)}{I^2(MA)\ R^2(m)} \qquad (19)$$

so that in ISX-B, for example, ($a = 0.27m$, $R = 0.93m$, $n = 7.10^{19}m^{-3}$) saturation effects would be expected to start when

$$P(MW) > 20\ I^2(MA)$$

which encompasses the usual operating range of this experiment.

Of course, if the scaling law (19) applied for indefinitely large input power, β would never saturate completely! However, as we have noted, a further degradation of confinement occurs at a much higher value of A, dependent on q_a. This effect of q_a on confinement cannot be well represented by a simple power law; rather it should be regarded as a limitation on the basic confinement scaling (18).

In discussing the ultimate β limits it is more convenient to consider β itself rather than β/β_c, and this is shown in Fig 7, which indicates the fully saturated β values reached as $P \to \infty$. (These are independent of the heating profile.) Fig 8 shows that these fully saturated values agree well with the expression given in reference [5] for the maximum stable β,

$$\beta_{max} = \frac{a}{5Rq} \qquad (20)$$

which was obtained as the best fit to extensive numerical stability

studies. It should be recalled that in the numerical calculations leading to equation (20) the q profile was essentially fixed while the pressure profile was optimised. In our model the q profile consistently adjusts, following Ohm's law, as the power input is increased and the pressure rises. It is therefore not a priori obvious that the two results for β_{max} should agree.

IV. Conclusions

We have introduced a simple transport model for high-β auxiliary heated tokamaks. In this model thermal conductivity has the form established for low-β ohmic discharges wherever the plasma is theoretically stable to mhd ballooning modes, but transport is essentially infinite where the profile is unstable to ballooning modes. It is also infinite within the $q = 1$ surface where sawtooth oscillations occur. With this model, confinement time and β can be calculated in terms of two parameters. The results show that there is a soft β-limit and a gradual degradation of confinement with input power. The onset of this degradation is predicted to occur within the range of present auxiliary heating experiments. When expressed as a confinement time scaling law, the results from our model are in very good agreement with the empirical scaling law reported for high β experiments, and the saturated β values also agree well with other computations. To this extent, therefore, it appears possible to account for the confinement in high-β, auxiliary heated, tokamaks in terms of the empirical law for confinement in low-β ohmic tokamaks - despite the apparent dissimilarity between the scaling laws for the two regimes.

References

[1] GOLDSTON, R, Proc 11th European Conference on Controlled Fusion and Plasma Physics, Aachen, 1983, Invited Paper.

[2] TODD, A M M, MANICKAM, J, OKABAYASHI, M, CHANCE, M S, GRIMM, R C, GREENE, J M, JOHNSON, J L, Nucl Fusion 19, 743 (1979).

[3] SYKES, A, TURNER, M F, FIELDING, P J, HAAS, F A, in Plasma Physics and Controlled Nuclear Fusion Research, Innsbruck, Austria, 1978 (IAEA, Vienna, 1979) Vol 1 p625.

[4] CONNOR, J W, HASTIE, R J, TAYLOR, J B, Phys Rev Letts 40, 396 (1978).

[5] SYKES, A, TURNER, M F, PATEL, S, 11th European Conference on Controlled Fusion and Plasma Physics, Aachen, 1983.

Figure Captions

Fig 1 The function $f(s)$ which governs ideal mhd ballooning instability

Fig 2 Variation of confinement time with input power: $h(x)$ = constant.

Fig 3 Variation of confinement time with input power: $h(x) = \exp(-2.77x^2)$.

Fig 4 Variation of β/β_c with input power: $h(x)$ = constant.

Fig 5 Variation of β/β_c with input power: $h(x) = \exp(-2.77x^2)$.

Fig 6a Log plot of confinement time against power: h = constant.

Fig 6b Log plot of confinement time against power: $h = \exp(-2.77x^2)$.

Fig 7 Variation of β with input power.

Fig 8 Comparison of saturated β values with published computations of β_{max}.

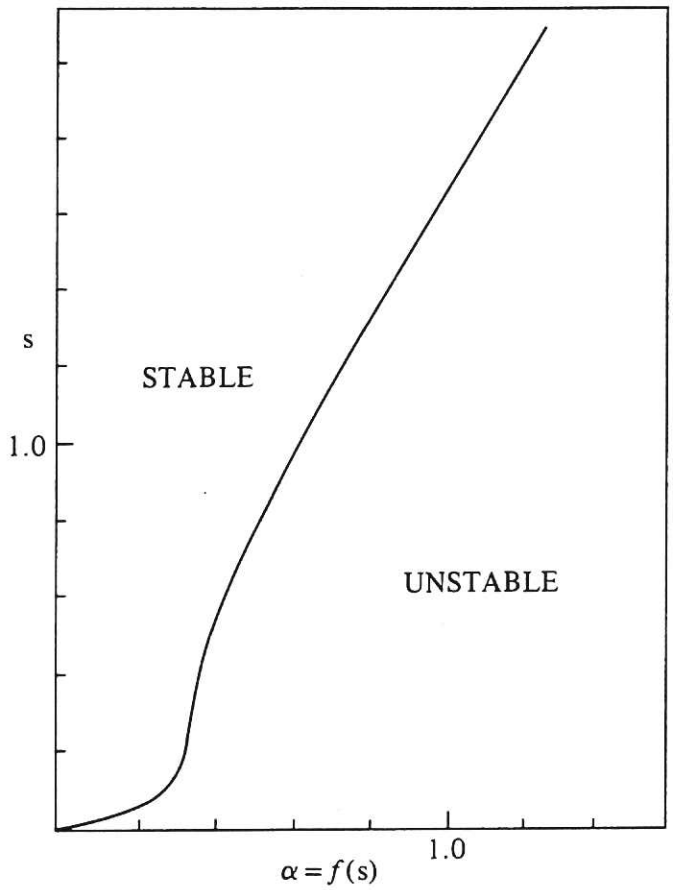

Fig.1 The function f(s) which governs ideal mhd ballooning instability.

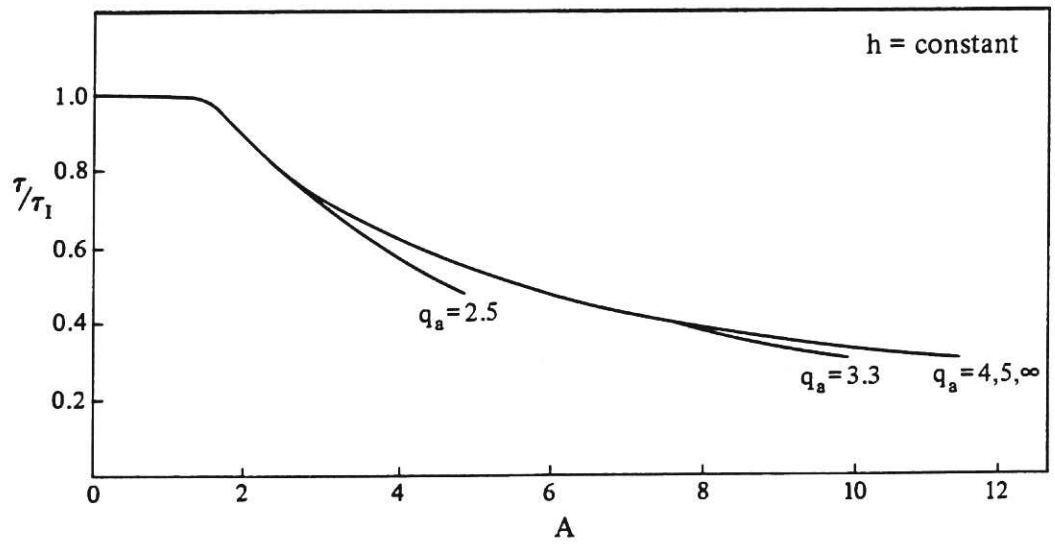

Fig.2 Variation of confinement time with input power: h(x) = constant.

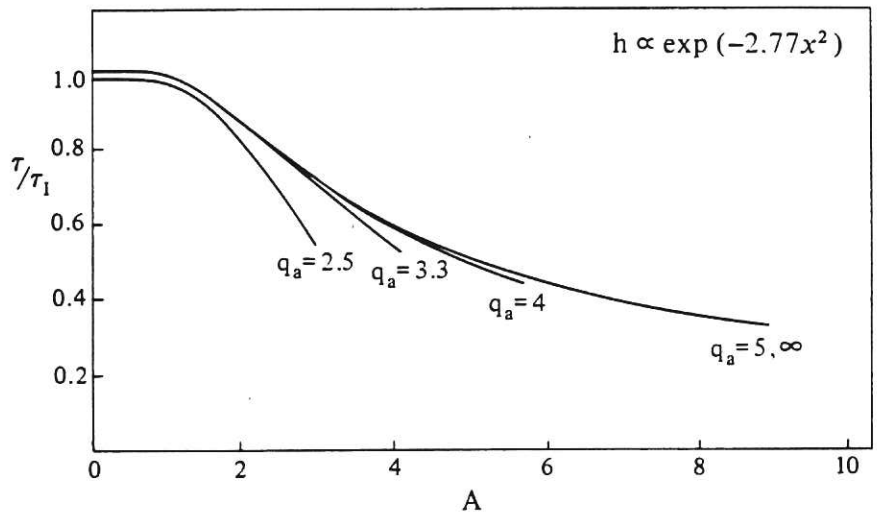

Fig.3 Variation of confinement time with input power: h(x) = exp(-2.77x²).

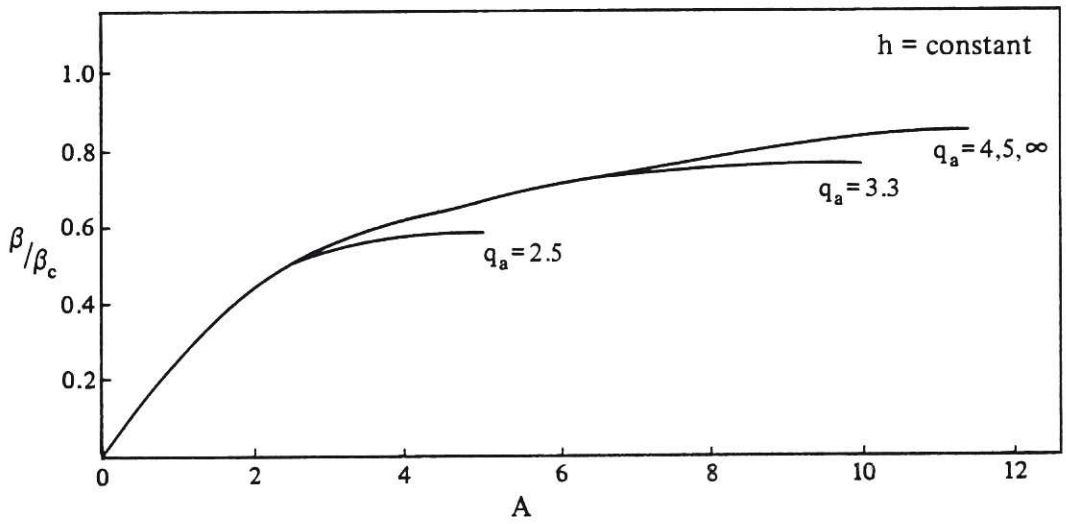

Fig.4 Variation of β/β_c with input power: h(x) = constant.

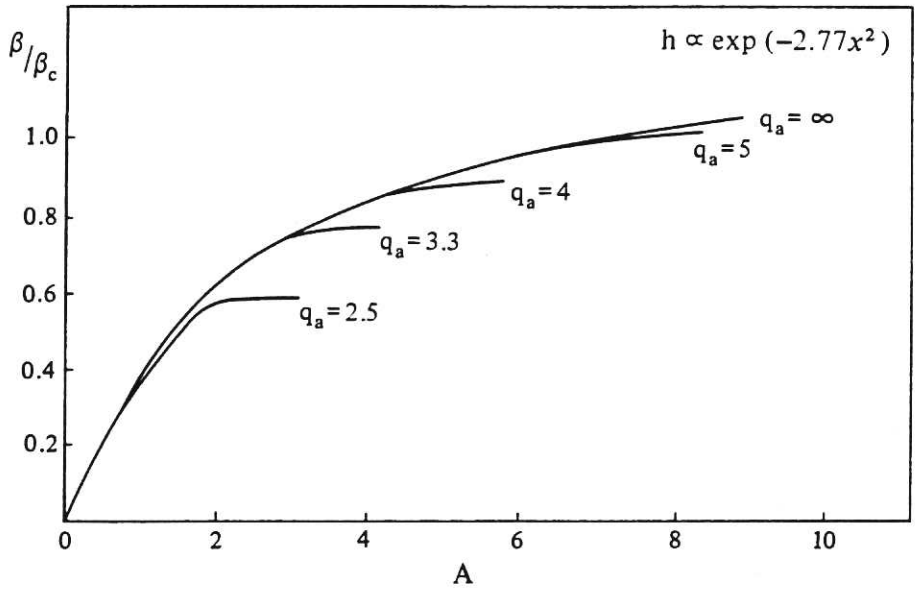

Fig.5 Variation of β/β_c with input power: h(x) = exp(−2.77x^2).

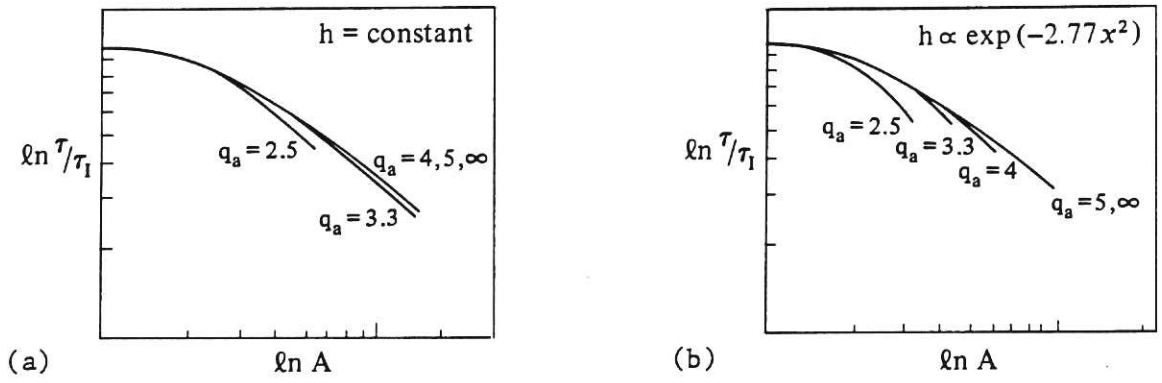

Fig.6a Log plot of confinement time against power: h = constant.
Fig.6b Log plot of confinement time against power: h = exp(−2.77x^2).

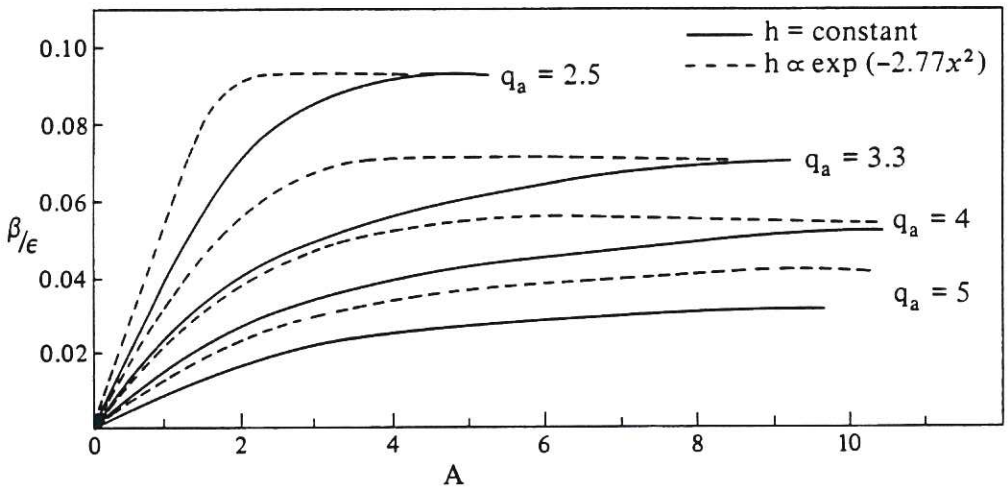

Fig.7 Variation of β with input power.

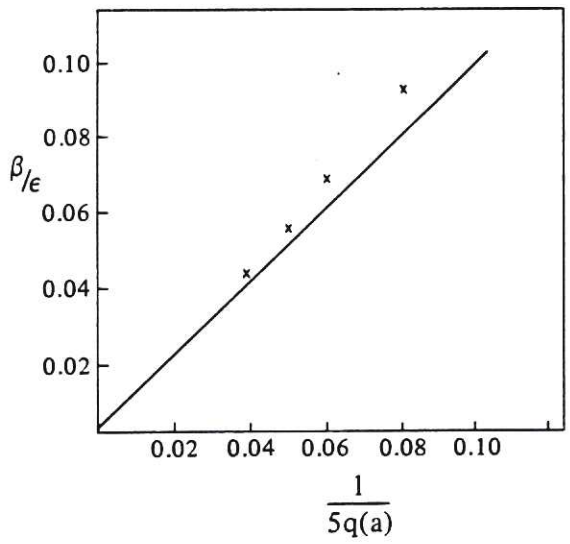

Fig.8 Comparison of saturated β values with published computations of β_{max}.